This article has been accepted for publication in a future issue of this journal, but has not been fully edited. Content may change prior to final publication. Citation information: DOI 10.1109/TWC.2015.2396052, IEEE Transactions on Wireless Communications

Optimum Power Allocation in Sensor Networks for Active Radar Applications

Gholamreza Alirezaei, *Member, IEEE,* Omid Taghizadeh, *Student Member, IEEE,* and Rudolf Mathar, *Member, IEEE*

***Abstract*—We investigate the power allocation problem in distributed sensor networks that are used for target object classification. In the classification process, the absence, the presence, or the type of a target object is observed by the sensor nodes independently. Since these local observations are noisy and thus unreliable, they are fused together as a single reliable observation at a fusion center. The fusion center uses the best linear unbiased estimator in order to accurately estimate the reflection coefficient of target objects. We utilize the average deviation between the estimated and the actual reflection coefficient as a metric for defining the objective function. First, we demonstrate that the corresponding optimization of the power allocation leads to a signomial program which is in general quite hard to solve. Nonetheless, by using the proposed system model, fusion rule and objective function, we are able to optimize the power allocation analytically and can hence present a closed-form solution. Since the power consumption of the entire network may be limited in various aspects, three different cases of power constraints are discussed and compared with each other. In addition, a sensitivity analysis of the optimal power allocation with respect to perfect and imperfect parameter knowledge is worked out.**

***Index Terms*—Analytical power allocation, energy-efficient optimization, distributed target classification, network resource management, information fusion.**

I. Introduction

In this paper, we investigate the power allocation problem in distributed sensor networks that are used for active radar applications. Each sensor node (SN) individually and independently emits a radar signal and receives the reflected echo from a jointly observed target object. The particular observations serve as classification feature in order to classify the type of the present target object. Since the local observations at each SN are noisy and thus unreliable, they are combined into a single reliable observation at a remotely located fusion center to increase the overall system performance. In the classification process, the absence, the presence, and the type of the present target object are distinguished. The fusion center uses the best linear unbiased estimator in order to accurately estimate the reflection coefficient of the present target object, where each object is assumed to be uniquely characterized by its reflection coefficient. This setup is illustrated in Figure 1, whose technical components will be specified in detail later.

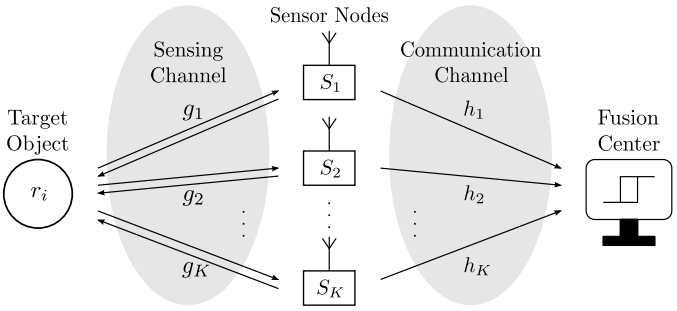

Fig. 1. Abstract representation of the distributed sensor network.

The research on distributed detection was originated from the attempt to combine signals of different radar devices [1]. Currently, distributed detection is rather discussed in the context of wireless sensor networks, where the sensor units may also be radar nodes [2]–[4]. In [5], the power allocation problem for distributed wireless sensor networks, which perform object detection and classification, is only treated for ultra-wide bandwidth (UWB) technology. Other applications, which require or benefit from detection and classification capabilities, are localization and tracking [6] or through-wall surveillance [7]. In [8], an approximate solution of the power allocation problem is proposed, which allows for an analytical treatment of output power-range limitation per sensor node. The optimal power allocation in passive radar systems, instead of active systems, is investigated in [9]. For active radar systems an optimal solution to the power allocation problem is only known for high signal-to-noise ratios (SNRs), see [10]. However, a closed-form optimal solution to the power allocation problem has not yet been investigated in the context of object classification for the whole range of SNR. The main difficulty for optimizing the power consumption is associated with finding a closed-form equation for the overall classification probability. As example, for the Bayesian hypothesis test criterion the overall classification probability cannot be analytically evaluated [11]. This limits the usability of this criterion for solving the power allocation problem. Bounds, such as the Bhattacharyya bound [12], are also difficult to use for optimizing multidimensional problems. Hence, the best power allocation scheme is still an open problem in order to improve the overall classification probability.

In the present work, we analytically optimize the power allocation and hence can present a closed-form solution for

Manuscript received January 28, 2014; first revision received June 21, 2014; second revision received November 26, 2014; accepted January 11, 2015. The associate editor coordinating the review of this paper and approving it for publication was Shuguang Cui.

All authors are with the Institute for Theoretical Information Technology, RWTH Aachen University, 52056 Aachen, Germany (e-mail: {alirezaei, taghizadeh, mathar}@ti.rwth-aachen.de).

This article has been accepted for publication in a future issue of this journal, but has not been fully edited. Content may change prior to final publication. Citation information: DOI 10.1109/TWC.2015.2396052, IEEE Transactions on Wireless Communications

a network of amplify-and-forward SNs. Based on a simple system model, we apply a linear fusion rule and utilize the average deviation between the estimated and the actual reflection coefficient as a metric for defining the objective function. This approach is the key idea in the present work which enables the analytical optimization of the power allocation in closed-form. Since the power consumption of the entire network may be limited in various aspects, three different cases of power constraints are discussed and compared with each other. They lead to explicit policies for the optimal power allocation. Furthermore, we demonstrate that all considered constraints lead to signomial optimization problems which are in general quite hard to solve. In addition, we simulatively analyze the sensitivity of the optimal objective with respect to perfect parameter knowledge and subsequently with respect to imperfect channel state information. These are the main contributions of the current work.

The present work is organized as follows. We start with a description of the underlying technical system in the next section. Subsequently, the power allocation problem is specified and analytically solved. The achieved results are then discussed and carefully compared with each other. Finally, simulative results are presented and their behavior is described.

Mathematical Notations:

Throughout this paper we denote the sets of natural, integer, real, and complex numbers by $\mathbb{N}$, $\mathbb{Z}$, $\mathbb{R}$, and $\mathbb{C}$, respectively. The imaginary unit is denoted by j. Note that the set of natural numbers does not include the element zero. Moreover, $\mathbb{R}_+$ denotes the set of non-negative real numbers. Furthermore, we use the subset $\mathbb{F}_N \subseteq \mathbb{N}$ which is defined as $\mathbb{F}_N \coloneqq \{1, \ldots, N\}$ for any given natural number N. We denote the absolute value of a real or complex-valued number z by $|z|$ while the expected value of a random variable v is denoted by $\mathcal{E}[v]$. Moreover, the notation $V^\star$ stands for the optimal value of an optimization variable V at an optimum point of the corresponding optimization problem.

II. Overview and Technical System Description

At any instance of time, a network of $K \in \mathbb{N}$ independent and spatially distributed SNs receives random observations. If a target object is present, then the received power at the SN S_k is a part of its own emitted power which is back-reflected from the jointly observed target object and is weighted by its reflection coefficient r_i. The object may be of I different types. It should be noted that sheer detection may be treated as the special case of $I = 2$ which corresponds to the decision '*some object is present*' versus '*there is no object*'. We assume that all different object types and their corresponding reflection coefficients are known by the network. Moreover, the received signal at each SN is weighted by the corresponding channel coefficient and disturbed by additive noise. It is obvious that the sensing channel is wireless. The sensing task and its corresponding communication task for a single classification process are performed in consecutive time slots. All SNs take samples from the disturbed received signal and amplify them without any additional data processing in each time slot.

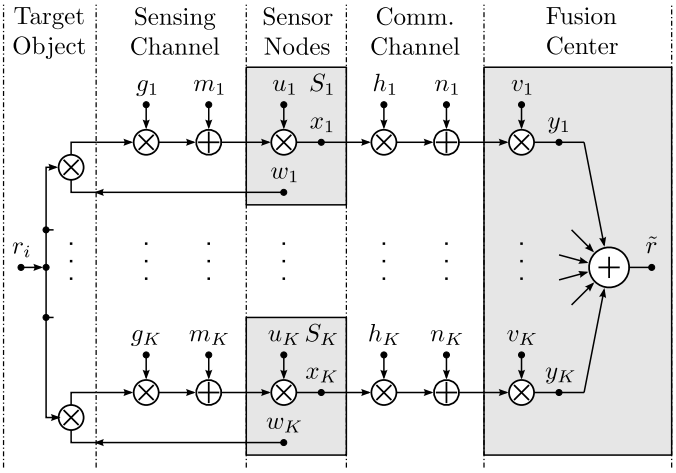

Fig. 2. System model of the distributed active sensor network.

The amplified samples remain buffered in the SNs during the current time slot. Simultaneously in the same time slot, new radio waves are emitted by all SNs for the next observation and classification process. In addition, the buffered samples of the former classification process are communicated to the fusion center which is placed in a remote location. We assume that SNs have only limited sum-power available for sensing the object and communicating to the fusion center. Furthermore, each SN may be limited in its transmission power-range due to transmission-power regulation standards or due to the functional range of its circuit elements. The sensing task as well as the communication to the fusion center are performed by using distinct waveforms (pulse shapes) for each SN so as to distinguish sensing and communication of different SNs. Each waveform has to be suitably chosen in order to suppress inter-user (inter-node) interference at other SNs and also at the fusion center. Furthermore, we assume that in the frequency domain each waveform is orthogonal to all other waveforms in order to calculate the sensing power of each SN independent from its communication power. Hence, the K received signals at the fusion center are uncorrelated and assumed to be conditionally independent. Each received signal at the fusion center is influenced by the corresponding channel coefficient and additive noise, as well. The communication channel between the SNs and the fusion center can either be wireless or wired. The disturbed received signals at the fusion center are weighted and combined together in order to obtain a single reliable observation $\tilde{r}$ of the actual reflection coefficient r_i. Note that we disregard time delays within all transmissions and assume synchronized data communication.

In the following subsections, we mathematically describe the underlying system model that is depicted in Figure 2. The continuous-time system is modeled by its discrete-time equivalent, where the sampling rate of the corresponding signals is equal to the target observation rate, for the sake of simplicity.

A. Target Object

We assume that all objects have the same size, shape and alignment, but different material and, hence, complex-valued

This article has been accepted for publication in a future issue of this journal, but has not been fully edited. Content may change prior to final publication. Citation information: DOI 10.1109/TWC.2015.2396052, IEEE Transactions on Wireless Communications

reflection coefficients $r_i \in \mathbb{C},\ i \in \mathbb{F}_I$. Thus, the reflection coefficients are the only recognition features in this work. The a-priori probability of occurrence for each object type is denoted by $\pi_i \in \mathbb{R}_+,\ i \in \mathbb{F}_I$, with $\sum_{i=1}^{I} \pi_i = 1$. The root mean squared value of the reflection coefficients is given as

$$r_{\text{rms}} \coloneqq \sqrt{\sum_{i \in \mathbb{F}_I} \pi_i \left| r_i \right|^2} \ . \tag{1}$$

Furthermore, the actual target object is assumed to be static during consecutive observation steps.

B. Sensing channel

Each propagation path of the sensing channel, from each SN to the object and again back to the same SN, is described by a corresponding random channel coefficient g_k. For the investigation of the power allocation problem, the concrete realization of channel coefficients is needed and hence can be used for postprocessing of the received signals at the SNs. We assume that all channel coefficients are complex-valued and static during each target observation step. Furthermore, the coherence time of sensing channels is assumed to be much longer than the whole length of the classification process. Thus, the expected value and the quadratic mean of each coefficient during each observation step can be assumed to be equal to their instantaneous values, i.e., $\mathcal{E}[g_k] = g_k$ and $\mathcal{E}[|g_k|^2] = |g_k|^2$. In practice, it is often difficult to measure or estimate these coefficients. Thus, the results of the present work are applicable for scenarios where all channel coefficients can somehow be accurately estimated during each observation process or they are nearly deterministic and thus can be measured before starting the radar task.

Furthermore, all channel coefficients are assumed to be uncorrelated and jointly independent. Note that each channel coefficient includes the radar cross section, the influence of the antenna, the impact of the filters, as well as all additional attenuation of the target signal.

At the input of each SN, the disturbance is modeled by the complex-valued additive white Gaussian noise (AWGN) m_k with zero mean and finite variance $M_0 \coloneqq \mathcal{E}[|m_k|^2]$ for all k. Note that the channel coefficient and the noise on the same propagation path are also uncorrelated and jointly independent.

C. Sensor nodes

We model each SN by an amplify-and-forward unit with extended capabilities, where both sensing and communication signals are transmitted simultaneously. The sensing signal w_k, without loss of generality, is assumed to be non-negative, real-valued and deterministic. The expected value of its sensing power is then described by

$$W_k \coloneqq \mathcal{E}[|w_k|^2] = |w_k|^2 \ , \ k \in \mathbb{F}_K \ . \tag{2}$$

Note that the specific value of w_k is adjustable and will be determined later by the power allocation procedure.

The ratio of the communication signal to the received signal is described by the non-negative real-valued amplification factor u_k which is assumed to be constant over the whole bandwidth and power-range. Thus, the communication signal and the expected value of its communication power are described by

$$x_k \coloneqq (r_i g_k w_k + m_k) u_k \ , \ k \in \mathbb{F}_K \tag{3}$$

and

$$X_k \coloneqq \mathcal{E}[|x_k|^2] = (r_{\text{rms}}^2 |g_k|^2 W_k + M_0) u_k^2 \ , \ k \in \mathbb{F}_K \ , \tag{4}$$

respectively. The amplification factor is an adjustable parameter and will be determined later by the power allocation procedure, as well. Note that the instantaneous power fluctuates from observation to observation depending on the present target object.

If the received signal is negligible in comparison to the output signal and if the nodes have smart power components with low-power dissipation loss, then the average power consumption of each node is approximately equal to its average output power $W_k + X_k$. The addition of both transmission powers is justified because the corresponding signals are assumed to be separated by distinct waveforms. We also assume that the output power-range of each SN is limited by P_{max} and that the average power consumption of all SNs together is limited by the sum-power constraint P_{tot}. Hence, the constraints

$$\begin{aligned} & W_k + X_k \leq P_{\text{max}} \\ & \Leftrightarrow \ \left(1 + r_{\text{rms}}^2 |g_k|^2 u_k^2\right) W_k + M_0 u_k^2 \leq P_{\text{max}} \ , \ k \in \mathbb{F}_K \end{aligned} \tag{5}$$

and

$$\begin{aligned} & \sum_{k \in \mathbb{F}_K} \underbrace{\underbrace{W_k}_{\text{Radar task}} + \underbrace{X_k}_{\text{Data communication}}}_{\text{Average transmission power of one sensor for a single observation}} \leq P_{\text{tot}} \\ & \Leftrightarrow \ \sum_{k \in \mathbb{F}_K} \left(1 + r_{\text{rms}}^2 |g_k|^2 u_k^2\right) W_k + M_0 u_k^2 \leq P_{\text{tot}} \end{aligned} \tag{6}$$

arise consequently. We remark that the described method can also be extended to individual output power-range constraints per SN.

Note that the sum-power constraint P_{tot} is a reasonable approach to compare energy-efficient radar systems.

D. Communication channel

Analogous to the sensing channel, each propagation path of the communication channel is described by a corresponding random channel coefficient h_k. But in contrast to the sensing channel, the concrete realization of each communication channel coefficient is measurable by using pilot sequences at each SN. Accordingly, the channel coefficients can be used for postprocessing of received signals at the fusion center. We assume that all channel coefficients are complex-valued and static during each target observation step. Furthermore, the coherence time of communication channels is also assumed to be much longer than the whole length of the classification process. Thus, the expected value and the quadratic mean of each channel coefficient can be assumed to be equal to their instantaneous values, i.e., $\mathcal{E}[h_k] = h_k$ and $\mathcal{E}[|h_k|^2] = |h_k|^2$. Furthermore, all channel coefficients are assumed to be uncorrelated and jointly independent. Note that each channel

This article has been accepted for publication in a future issue of this journal, but has not been fully edited. Content may change prior to final publication. Citation information: DOI 10.1109/TWC.2015.2396052, IEEE Transactions on Wireless Communications

coefficient includes the influence of the antenna, the impact of the filters, as well as all additional attenuation of the corresponding sensor signal.

At the input of the fusion center, the disturbance on each communication path is modeled by the complex-valued AWGN n_k with zero mean and finite variance $N_0 \coloneqq \mathcal{E}[|n_k|^2]$ for all k. Note that the channel coefficient and the noise on the same propagation path are also uncorrelated and jointly independent.

E. Fusion center

The fusion center combines the different local observations into a single reliable one by applying a linear combiner. Thus, the received signals are weighted with the complex-valued factors v_k and summed up to yield an estimate $\tilde{r}$ of the actual target signal r_i. In this way, we obtain

$$y_k \coloneqq (x_k h_k + n_k) v_k \,, \;\; k \in \mathbb{F}_K \,, \tag{7}$$

and hence,

$$\tilde{r} \coloneqq \sum_{k \in \mathbb{F}_K} y_k = r_i \sum_{k \in \mathbb{F}_K} w_k g_k u_k h_k v_k + \sum_{k \in \mathbb{F}_K} (m_k u_k h_k + n_k) v_k \,. \tag{8}$$

Note that each weight can be written as $v_k = |v_k| \exp(\mathrm{j}\,\vartheta_k)$, $k \in \mathbb{F}_K$, where ϑ_k is a real-valued number which represents the phase of the corresponding weight.

Note that the fusion center can separate the input streams because the communication channel is either wired or the data communication is performed by distinct waveforms for each SN. Consequently, if the communication channel is wireless then a matched-filter bank is essential at the input of the fusion center to separate the data streams of different SNs. In addition, we do not consider inter-user (inter-node) interferences at the fusion center because of the distinct waveform choices.

In order to obtain a single reliable observation at the fusion center, the value $\tilde{r}$ should be a good estimate for the present reflection coefficient r_i. Thus, we optimize the sensing power W_k, the amplification factors u_k, and the weights v_k in order to minimize the average absolute deviation between $\tilde{r}$ and the true reflection coefficient r_i. This optimization procedure is elaborately explained in the next section. After determining W_k, u_k and v_k, the fusion center observes a disturbed version of the true reflection coefficient r_i at the input of its decision unit. Hence, by using the present system model, we are able to separate the power allocation problem from the classification problem and optimize both independently.

F. Some remarks on the system model

All described assumptions are necessary to obtain a framework suitable for analyzing the power allocation problem, without studying detection, classification and estimation problems in specific systems and their settings.

The accurate estimation of all channel coefficients is necessary for both the radar process and the power allocation. Sometimes it is not possible to estimate the transmission channels; consequently the channel coefficients g_k and h_k remain unknown. In such cases, the radar usually fails to perform its task.

TABLE I
NOTATION OF SYMBOLS THAT ARE NEEDED FOR THE DESCRIPTION OF EACH OBSERVATION PROCESS.

Notation	Description
K	number of all nodes;
$\mathbb{F}_K$	the index-set of K nodes;
$\tilde{K}$	number of all active nodes;
$\mathbb{K}$	the index-set of all active nodes;
I	number of different reflection coefficients;
r_i	reflection coefficient of i^{th} target object;
r_{rms}	root mean squared absolute value of reflection coefficients;
$\tilde{r}$	estimate of the actual reflection coefficient r_i;
g_k, h_k	complex-valued channel coefficients;
m_k, n_k	complex-valued zero-mean AWGN;
M_0, N_0	variances of m_k and n_k;
u_k, v_k	non-negative amplification factors and complex-valued weights;
ϑ_k	phase of v_k;
ϕ_k	phase of the product $g_k \cdot h_k$;
w_k, x_k	sensing and communication signal of k^{th} sensor node;
W_k, X_k	sensing and communication power of k^{th} sensor node;
y_k	input signals of the combiner;
P_{max}	output power-range constraint of each sensor node;
P_{tot}	sum-power constraint.

Since the channel coefficients g_k are in practice difficult to estimate or to determine, our approach rather shows theoretical aspects of the power allocation than the practical realization and implementation. Hence, the presented results act as theoretical bounds and references for comparing real radar systems.

Moreover, since the coherence time of communication channels as well as sensing channels is assumed to be much longer than the whole length of the classification process, the proposed power allocation method is applicable only for scenarios with slow-fading channels.

Note that only the linear fusion rule together with the proposed objective function enable optimizing the power allocation in closed-form. The optimization of power allocation in other cases is in general hardly amenable analytically.

In general, SNs have only one power amplifier and a single antenna. The antenna is usually connected to a circulator in order to separate the signal of the transmitter to the antenna from the signal of the antenna to the receiver, which is not depicted in Figure 2. The power amplifier is also shared for sensing and communication tasks, but not considered in this work.

In order to increase the available power-range at each SN, time-division multiple-access (TDMA) can be used to completely separate the sensing task from the communication task and perform each task in a different time slot.

The introduced system model describes a baseband communication system without considering time, phase and frequency synchronization problems.

In order to distinguish the current operating mode of each SN in what follows, we say a SN is *inactive* or *idle* if the allocated power is zero. We say a SN is *active* if its allocated power is positive. Finally, we say a SN is *saturated* if the limitation of its output power-range is equal to the allocated power, i.e., $P_{\text{max}} = W_k + X_k$.

An overview of all notations that we will use hereinafter and are needed for the description of each observation process is depicted in Table I.

This article has been accepted for publication in a future issue of this journal, but has not been fully edited. Content may change prior to final publication. Citation information: DOI 10.1109/TWC.2015.2396052, IEEE Transactions on Wireless Communications

III. Power Allocation

In this section, we introduce the power optimization problem and consecutively present its analytical solutions for different power constraints. First, we investigate the case where only a sum-power constraint $P_{\text{tot}} \in \mathbb{R}_+$ for the cumulative sum of the expected power consumption of each SN is given. Afterwards, we present the analytical solution of the power allocation problem for the case where the average transmission power of each SN is limited by the output power-range limitation $P_{\text{max}} \in \mathbb{R}_+$. Finally, we extend the power allocation problem to the case where both constraints simultaneously hold and present the corresponding optimal solution.

In general, the objective is to maximize the overall classification probability, however, a direct solution to the allocation problem does not exist, since no analytical expression for the overall classification probability is available. Instead, we minimize the average deviation between $\tilde{r}$ and r_i, in order to determine the power allocation. The motivation for this method is the separation of the power allocation problem from the object classification procedure, as described in the last section. The corresponding optimization problem is elaborately described in the next subsection.

A. The optimization problem

As mentioned in the last section, the value $\tilde{r}$ should be a good estimate for the actual reflection coefficient r_k of the present target object. In particular, we aim at finding estimators $\tilde{r}$ of minimum mean squared error in the class of unbiased estimators for each i.

The estimate $\tilde{r}$ is unbiased simultaneously for each i if $\mathcal{E}[\tilde{r} - r_i] = 0$, i.e., from equation (8) with (2) we obtain the identity

$$\sum_{k \in \mathbb{F}_K} \sqrt{W_k}\, g_k u_k h_k v_k = 1\,. \tag{9}$$

This identity is our first constraint in what follows. Note that the mean of the second sum in (8) vanishes since the noise is zero-mean. Furthermore, we do not consider the impact of both random variables g_k and h_k as well as their estimates in our calculations because the coherence time of both channels is assumed to be much longer than the target observation time. Note that equation (9) is complex-valued and may be separated as

$$\sum_{k \in \mathbb{F}_K} \sqrt{W_k}\, u_k \, |v_k g_k h_k| \cos(\vartheta_k + \phi_k) = 1 \tag{10}$$

and

$$\sum_{k \in \mathbb{F}_K} \sqrt{W_k}\, u_k \, |v_k g_k h_k| \sin(\vartheta_k + \phi_k) = 0\,, \tag{11}$$

where ϑ_k and ϕ_k are phases of v_k and $g_k h_k$, respectively.

The objective is to minimize the mean squared error $\mathcal{E}[|\tilde{r} - r_i|^2]$. By using equation (8) and the identity (9) we may write the objective function as

$$V \coloneqq \mathcal{E}\big[|\tilde{r} - r_i|^2\big] = \sum_{k \in \mathbb{F}_K} |v_k|^2 \big(u_k^2 |h_k|^2 M_0 + N_0\big)\,. \tag{12}$$

Note that (12) is only valid if m_k and n_k are white and jointly independent.

As mentioned in the last section, each SN has an output power-range limitation and the expected overall power consumption is also limited. Hence, the objective function is also subject to (5) and (6), which are our second and last constraints, respectively.

In summary, the optimization problem is to minimize the mean squared error in (12) with respect to u_k, v_k, and W_k, subject to constraints (5), (6), (10) and (11).

Note that each resulting optimization problem is a *signomial program*, which is a generalization of *geometric programming*, and is thus non-convex in general [13]. Furthermore, it is important to note that signomial programs cannot be transformed in general into convex optimization problems [14]. Since we have not found any transformation from signomials into corresponding convex programs thus far, we hence apply the general method of Lagrangian multipliers with equality constraints to solve all optimization problems in the present work, see [15, pp. 321–358] and [16, pp. 275–368]. In order to ensure the global optimality of our results, we consecutively show the following four steps during each solving procedure. First, we relax each problem into an optimization problem with extended ranges for all involved variables to ensure an optimization within the *interior-set*. Second, all stationary points of the associated Lagrangian are localized by considering the corresponding derivatives to obtain *necessary* conditions. Third, we show that the number of stationary points is equal to one, which indirectly implies that the considered stationary point is also a *regular* point for all (active) constraints. Finally, to obtain a *sufficient* condition, we then show that the stationary point has a convex neighborhood which corresponds with a minimum. In summary, the applied method is based on the regularity of all active constraints as well as first and second order optimality conditions which together guarantee for global optimality. At this point, we emphasize that obtaining global optimality is similarly achievable by applying vector space methods [17], using interval analysis [18], or utilizing a proper constraint qualification (CQ) together with Karush-Kuhn-Tucker conditions (KKT) [19].

B. Power allocation subject to the sum-power constraint

In this case, the output power-range constraint per SN is assumed to be greater than the sum-power constraint and thus does not have any effect on the optimization problem, because the feasible set of the optimization problem is only limited by the sum-power constraint. This leads to the corresponding constrained Lagrange function (relaxation with respect to the range of W_k, u_k and $|v_k|$)

$$\begin{aligned} L_1(W_k, u_k, v_k; \eta_1, \eta_2, \tau; \xi) \coloneqq{}& \sum_{k \in \mathbb{F}_K} |v_k|^2 \left(u_k^2 |h_k|^2 M_0 + N_0\right) \\ &+ \left(1 - \sum_{k \in \mathbb{F}_K} \sqrt{W_k} u_k \, |v_k g_k h_k| \cos(\vartheta_k + \phi_k)\right)\eta_1 \\ &- \left(\sum_{k \in \mathbb{F}_K} \sqrt{W_k} u_k \, |v_k g_k h_k| \sin(\vartheta_k + \phi_k)\right)\eta_2 \\ &+ \left(P_{\text{tot}} - \xi - \sum_{k \in \mathbb{F}_K} \left(1 + r_{\text{rms}}^2 |g_k|^2 u_k^2\right) W_k + M_0 u_k^2\right)\tau\,, \end{aligned} \tag{13}$$

This article has been accepted for publication in a future issue of this journal, but has not been fully edited. Content may change prior to final publication. Citation information: DOI 10.1109/TWC.2015.2396052, IEEE Transactions on Wireless Communications

where η_1, η_2 and τ are Lagrange multipliers while ξ is a slack variable.

In order to satisfy (11), all phases $\vartheta_k + \phi_k$ have to be equal to $q_k\pi$, $q_k \in \mathbb{Z}$, for all $k \in \mathbb{F}_K$. If there were a better solution for $\vartheta_k + \phi_k$, then the first partial derivatives of L_1 with respect to ϑ_k would vanish at that solution, due to the continuity of trigonometric functions. But the first derivatives would lead to the equations $\eta_1 \sin(\vartheta_k + \phi_k) = \eta_2 \cos(\vartheta_k + \phi_k)$ which cannot simultaneously satisfy both equations (10) and (11) for all η_1 and η_2. Thus, $q_k\pi$ is the unique solution. Hence, we may consequently write a modified Lagrange function as

$$\begin{aligned}\tilde{L}_1(W_k, u_k, |v_k|, q_k; \eta_1, \tau; \xi) &\coloneqq \sum_{k\in\mathbb{F}_K} |v_k|^2 \left(u_k^2 |h_k|^2 M_0 + N_0\right) \\ &+ \left(1 - \sum_{k\in\mathbb{F}_K} \sqrt{W_k} u_k \, |v_k g_k h_k| \cos(q_k\pi)\right)\eta_1 \\ &+ \left(P_{\text{tot}} - \xi - \sum_{k\in\mathbb{F}_K} \left(1 + r_{\text{rms}}^2 |g_k|^2 u_k^2\right) W_k + M_0 u_k^2\right)\tau \,. \end{aligned} \tag{14}$$

At any stationary point of $\tilde{L}_1$ the first partial derivatives of $\tilde{L}_1$ with respect to W_k, u_k, $|v_k|$, η_1 and τ must vanish, if they exist. For all $l \in \mathbb{F}_K$, this leads to

$$\begin{aligned}\frac{\partial \tilde{L}_1}{\partial W_l} &= -\frac{u_l \, |v_l h_l g_l| \cos(q_l\pi)}{2\sqrt{W_l}}\eta_1 \\ &\quad - \left(1 + r_{\text{rms}}^2 |g_l|^2 u_l^2\right)\tau = 0 \,, \end{aligned} \tag{15}$$

$$\begin{aligned}\frac{\partial \tilde{L}_1}{\partial |v_l|} &= 2|v_l|\left(u_l^2 |h_l|^2 M_0 + N_0\right) \\ &\quad - \sqrt{W_l} u_l \, |h_l g_l| \cos(q_l\pi)\eta_1 = 0 \,, \end{aligned} \tag{16}$$

$$\begin{aligned}\frac{\partial \tilde{L}_1}{\partial u_l} &= 2|v_l|^2 u_l |h_l|^2 M_0 - \sqrt{W_l} \, |v_l h_l g_l| \cos(q_l\pi)\eta_1 \\ &\quad - 2u_l(W_l r_{\text{rms}}^2 |g_l|^2 + M_0)\tau = 0 \,, \end{aligned} \tag{17}$$

$$\frac{\partial \tilde{L}_1}{\partial \eta_1} = 1 - \sum_{k\in\mathbb{F}_K} \sqrt{W_k} u_k |v_k g_k h_k| \cos(q_k\pi) = 0 \tag{18}$$

and

$$\frac{\partial \tilde{L}_1}{\partial \tau} = P_{\text{tot}} - \xi - \sum_{k\in\mathbb{F}_K} \left(1 + r_{\text{rms}}^2 |g_k|^2 u_k^2\right) W_k + M_0 u_k^2 = 0 \,. \tag{19}$$

By multiplying (16) with $|v_l|$, summing up the outcome over all l, and using the identities (10) and (12), we obtain

$$\eta_1 = 2V \tag{20}$$

which is a positive real number due to definition of V. Because of the last relationship and according to (16), the value of $\cos(q_l\pi)$ must be a positive number and hence each q_l must be an even integer number. Thus, we can choose $q_l^\star = 0$ for all $l \in \mathbb{F}_K$ and conclude

$$\vartheta_l^\star = -\phi_l \,, \; l \in \mathbb{F}_K \,. \tag{21}$$

This solution gives the identity $\cos(q_l^\star\pi) = 1$ which can be incorporated into (15), (16), (17) and (18).

Again by multiplying (16) with

$$\frac{1}{2} \frac{u_l |h_l g_l| \sqrt{W_l}}{u_l |h_l|^2 M_0 + N_0} \,, \tag{22}$$

summing up the outcome over all l, and using (10), (12) and (20), we obtain

$$V = \frac{\eta_1}{2} = \left[\sum_{k\in\mathbb{F}_K} \frac{u_k^2 |h_k g_k|^2 W_k}{u_k^2 |h_k|^2 M_0 + N_0}\right]^{-1} . \tag{23}$$

In turn, by incorporating (23) into (16), it yields

$$|v_l| = \frac{V u_l |h_l g_l| \sqrt{W_l}}{u_l^2 |h_l|^2 M_0 + N_0} \tag{24}$$

for all $l \in \mathbb{F}_K$.

Note that for each feasible u_l and W_l, $l \in \mathbb{F}_K$, equation (24) describes a feasible value for each $|v_l|$. Since for each $u_l W_l > 0$ the relation $|v_l| > 0$ consequently follows, the feasible optimal values of each $|v_l| > 0$ are not on the boundary $|v_l| = 0$. Thus, finding optimal values for each u_l and W_l, $l \in \mathbb{F}_K$, leads to optimum values for each $|v_l|$, $l \in \mathbb{F}_K$, due to the convexity of (14) with respect to each $|v_l|$. Hence, finding a unique global optimum for u_l and W_l, $l \in \mathbb{F}_K$, yields the sufficient condition for the globally optimal solution of the minimization problem (14).

We replace each $|v_l|$ in (15) and (17) with (24) and thus we obtain two equations for τ as

$$\tau = \frac{-V^2 u_l^2 |g_l h_l|^2}{\left(1 + u_l^2 r_{\text{rms}}^2 |g_l|^2\right)\left(u_l^2 |h_l|^2 M_0 + N_0\right)} \tag{25}$$

and

$$\tau = \frac{-V^2 W_l |g_l h_l|^2 N_0}{\left(W_l r_{\text{rms}}^2 |g_l|^2 + M_0\right)\left(u_l^2 |h_l|^2 M_0 + N_0\right)^2} \,. \tag{26}$$

Note that because of the negativity of τ, due to (25) or (26), and positivity of η_1, the Lagrangian (14) is also convex in both u_l and W_l, $l \in \mathbb{F}_K$, as well. Hence, this Lagrangian is convex near any optimum/stationary point in each u_l, $|v_l|$ and W_l, but it seems not to be a jointly convex function, at all. Since this Lagrangian is separately convex in each direction, a possible stationary point can never be a maximum. As the derivatives in (15)–(19) are linear or at most quadratic separately for each variable, we will see later that only a single feasible stationary point exists.

For the sake of simplicity and in order to compare the results later on, we define new quantities as

$$\alpha_k \coloneqq \frac{M_0}{r_{\text{rms}}^2 |g_k|^2} \;\Rightarrow\; \alpha_k \in \mathbb{R}_+ \,, \tag{27}$$

$$\beta_k \coloneqq \frac{N_0}{|h_k|^2} \;\Rightarrow\; \beta_k \in \mathbb{R}_+ \,, \tag{28}$$

and

$$\tilde{u}_k \coloneqq M_0 u_k^2 \;\Leftrightarrow\; u_k = +\sqrt{\frac{\tilde{u}_k}{M_0}} \,. \tag{29}$$

By direct algebra from (25) and (26), we infer

$$W_l = \frac{\tilde{u}_l \alpha_l (\tilde{u}_l + \beta_l)}{\alpha_l \beta_l - \tilde{u}_l^2} \,, \; l \in \mathbb{F}_K \,. \tag{30}$$

This article has been accepted for publication in a future issue of this journal, but has not been fully edited. Content may change prior to final publication. Citation information: DOI 10.1109/TWC.2015.2396052, IEEE Transactions on Wireless Communications

To satisfy the positivity of each W_l, the inequality

$$\alpha_l\beta_l > \tilde{u}_l^2\,,\ l \in \mathbb{F}_K\,, \tag{31}$$

must hold, which will be used later. By using (27)–(30), we may rewrite (19) and (23) as

$$1 = (P_{\text{tot}} - \xi)\Bigg[\sum_{k\in\mathbb{F}_K} \underbrace{\frac{\tilde{u}_k^2(\alpha_k+\beta_k)+2\tilde{u}_k\alpha_k\beta_k}{\alpha_k\beta_k-\tilde{u}_k^2}}_{=:\gamma_k}\Bigg]^{-1} \tag{32}$$

and

$$V^{-1} = \frac{1}{r_{\text{rms}}^2}\sum_{k\in\mathbb{F}_K}\frac{\tilde{u}_k^2}{\alpha_k\beta_k-\tilde{u}_k^2} \tag{33}$$

respectively. In turn, we incorporate (32) into (33) and infer

$$V^{-1} = \frac{P_{\text{tot}}-\xi}{r_{\text{rms}}^2\sum_{k\in\mathbb{F}_K}\gamma_k}\sum_{k\in\mathbb{F}_K}\frac{\gamma_k\tilde{u}_k}{\tilde{u}_k(\alpha_k+\beta_k)+2\alpha_k\beta_k}\,. \tag{34}$$

As is well-known, the arithmetic mean in (34) is less than its greatest element such that the inequality

$$V^{-1} \le \frac{P_{\text{tot}}-\xi}{r_{\text{rms}}^2}\max_{k\in\mathbb{F}_K}\Big\{\frac{\tilde{u}_k}{\tilde{u}_k(\alpha_k+\beta_k)+2\alpha_k\beta_k}\Big\} \tag{35}$$

arises consequently. It is obvious that (35) is strictly decreasing with respect to ξ. Thus, the optimal value for the slack variable is zero, i.e., $\xi^\star = 0$. In (35), equality holds, if and only if, some elements are zero and all other ones are equal. In addition, it is obvious that (35) is strictly increasing in each $\tilde{u}_k$ and in turn the maximum value of a certain $\tilde{u}_k$ is achieved if for all $l \neq k$, $l \in \mathbb{F}_K$, the identity $\tilde{u}_l = 0$ holds, since the sum-power is kept constant. This means that only one SN is active and all other ones are idle. Hence, we can calculate the value of the corresponding $\tilde{u}_k$ from (32) as

$$\tilde{u}_k = \sqrt{\Big(\frac{\alpha_k\beta_k}{\alpha_k+\beta_k+P_{\text{tot}}}\Big)^2+\frac{\alpha_k\beta_k P_{\text{tot}}}{\alpha_k+\beta_k+P_{\text{tot}}}} - \frac{\alpha_k\beta_k}{\alpha_k+\beta_k+P_{\text{tot}}}\,. \tag{36}$$

This value can be incorporated into (35) to obtain

$$V^{-1} = \frac{P_{\text{tot}}^2}{r_{\text{rms}}^2}\max_{k\in\mathbb{F}_K}\Big\{\frac{1}{c_k^2(P_{\text{tot}})-P_{\text{tot}}^2}\Big\} \tag{37}$$

with the *disturbance-intensity*[1]

$$c_k(P) \coloneqq \sqrt{\alpha_k\beta_k}+\sqrt{(\alpha_k+P)(\beta_k+P)}\,,\ k\in\mathbb{F}_K, P\in\mathbb{R}_+\,. \tag{38}$$

The value of V^{-1} is maximal if the disturbance-intensity $c_k(P_{\text{tot}})$ is minimal. Hence, we re-index all SNs such that the inequality chain

$$c_k(P_{\text{tot}}) \le c_{k+1}(P_{\text{tot}})\ ,\ k\in\mathbb{F}_{K-1}\,, \tag{39}$$

holds and with that only the first SN is active, even if the first few disturbance-intensities are equal. From (24), (29), (30), (36) and (37) we thus conclude

$$V^\star = \frac{r_{\text{rms}}^2}{P_{\text{tot}}^2}\big(c_1^2(P_{\text{tot}})-P_{\text{tot}}^2\big)\,, \tag{40}$$

$$\tilde{u}_1^\star = \sqrt{\Big(\frac{\alpha_1\beta_1}{\alpha_1+\beta_1+P_{\text{tot}}}\Big)^2+\frac{\alpha_1\beta_1P_{\text{tot}}}{\alpha_1+\beta_1+P_{\text{tot}}}} - \frac{\alpha_1\beta_1}{\alpha_1+\beta_1+P_{\text{tot}}}\,, \tag{41}$$

$$u_1^\star = \sqrt{\frac{\tilde{u}_1^\star}{M_0}}\,, \tag{42}$$

$$W_1^\star = \frac{\tilde{u}_1^\star\alpha_1(\tilde{u}_1^\star+\beta_1)}{\alpha_1\beta_1-(\tilde{u}_1^\star)^2}\,, \tag{43}$$

$$|v_1^\star| = \frac{V^\star\tilde{u}_1^\star}{r_{\text{rms}}|h_1|\sqrt{\tilde{u}_1^\star+\beta_1}\sqrt{\alpha_1\beta_1-(\tilde{u}_1^\star)^2}}\,, \tag{44}$$

and

$$|v_k^\star| = W_k^\star = u_k^\star = 0\,,\ k\in\mathbb{F}_K,\, k\neq 1\ . \tag{45}$$

As mentioned before, the Lagrangian (14) is separately convex in each direction, such that possible stationary points cannot be maximum ones. On the other hand, as shown in (40)–(45), there exists only a single feasible solution for the set of derivatives in (15)–(19). This means that only a single stationary point exists which cannot be a maximum. To be a saddle point is also not possible, because then there would at least exist one additional stationary point which is not the case here. Thus, the Lagrangian (14) must actually be a jointly convex function in the neighborhood of its stationary point. Furthermore, since the number of stationary points is equal to one, all equality (active) constraints are regular. Hence, the separate convexity together with the regularity condition is even a sufficient condition for global optimality in the present case, see also [15]. Note also that all above results are the solution of the relaxed Lagrangian (13) with extended range of all variables, and nevertheless this solution coincides with the original range of all variables.

Note that by using the above results, the corresponding fusion rule is simplified by discarding the influence of inactive SNs from the fusion rule. The fusion rule (8) becomes

$$\tilde{r} = y_1 = r_i + (m_1h_1u_1^\star+n_1)v_1^\star\,,\ i\in\mathbb{F}_I\ . \tag{46}$$

The equations (40)–(45) and (21) are the optimal solutions of the power allocation problem only subject to the sum-power constraint. They are hence the main contribution of the present subsection.

C. Power allocation subject to individual power constraints

In the current case, the sum-power constraint is assumed to be much greater than the output power-range constraint and thus does not have any effect on the optimization problem, because the feasible set of the optimization problem is only limited by the output power-range constraints. This leads to the corresponding constrained Lagrange function (relaxation

[1]We give the name disturbance-intensity to c_k because it behaves intrinsically like a metric for noise. Since $1/c_k$ also describes the quality of the k^{th} SN, it can be interpreted as its reliability, see [20].

This article has been accepted for publication in a future issue of this journal, but has not been fully edited. Content may change prior to final publication. Citation information: DOI 10.1109/TWC.2015.2396052, IEEE Transactions on Wireless Communications

with respect to the range of W_k, u_k and $|v_k|$)

$$\begin{aligned} &L_2(W_k, u_k, v_k; \eta_1, \eta_2, \lambda_k; \varrho_k) \\ &\quad := \sum_{k\in\mathbb{F}_K} |v_k|^2 \left(u_k^2 |h_k|^2 M_0 + N_0\right) \\ &\quad + \Bigg(1 - \sum_{k\in\mathbb{F}_K} \sqrt{W_k} u_k \, |v_k g_k h_k| \cos(\vartheta_k + \phi_k)\Bigg)\eta_1 \\ &\quad - \Bigg(\sum_{k\in\mathbb{F}_K} \sqrt{W_k} u_k \, |v_k g_k h_k| \sin(\vartheta_k + \phi_k)\Bigg)\eta_2 \\ &\quad + \sum_{k\in\mathbb{F}_K} \Big(P_{\max} - \varrho_k - \big(1 + r_{\text{rms}}^2 |g_k|^2 u_k^2\big) W_k - M_0 u_k^2\Big)\lambda_k \,, \end{aligned} \tag{47}$$

where λ_k are new Lagrange multipliers while ϱ_k are new slack variables.

Since the behavior of L_2 is identical to that of L_1 with respect to $|v_k|$ and ϑ_k, we obtain the same results for the phases as given in (21). Hence, we may modify L_2 as

$$\begin{aligned} &\tilde{L}_2(W_k, u_k, |v_k|\,; \eta_1, \lambda_k; \varrho_k) \\ &\quad := \sum_{k\in\mathbb{F}_K} |v_k|^2 \left(u_k^2 |h_k|^2 M_0 + N_0\right) \\ &\quad + \Bigg(1 - \sum_{k\in\mathbb{F}_K} \sqrt{W_k} u_k \, |v_k g_k h_k|\Bigg)\eta_1 \\ &\quad + \sum_{k\in\mathbb{F}_K} \Big(P_{\max} - \varrho_k - \big(1 + r_{\text{rms}}^2 |g_k|^2 u_k^2\big) W_k - M_0 u_k^2\Big)\lambda_k \,. \end{aligned} \tag{48}$$

Note that since the equality $\sin(\vartheta_k^\star + \phi_k) = 0$ holds due to (21), the constraint (11) is discarded in (48).

At any stationary point of $\tilde{L}_2$ the first partial derivatives of $\tilde{L}_2$ with respect to W_k, u_k, $|v_k|$, η_1 and λ_k must vanish, if they exist. For all $l \in \mathbb{F}_K$, this leads to

$$\frac{\partial \tilde{L}_2}{\partial W_l} = -\frac{u_l |v_l h_l g_l|}{2\sqrt{W_l}}\eta_1 - \big(1 + u_l^2 r_{\text{rms}}^2 |g_l|^2\big)\lambda_l = 0 \,, \tag{49}$$

$$\frac{\partial \tilde{L}_2}{\partial\, |v_l|} = 2\,|v_l| \left(u_l^2 |h_l|^2 M_0 + N_0\right) - \sqrt{W_l} u_l |h_l g_l| \eta_1 = 0 \,, \tag{50}$$

$$\begin{aligned} \frac{\partial \tilde{L}_2}{\partial u_l} &= 2|v_l|^2 u_l |h_l|^2 M_0 - \sqrt{W_l} |v_l h_l g_l| \eta_1 \\ &\quad - 2u_l \big(W_l r_{\text{rms}}^2 |g_l|^2 + M_0\big)\lambda_l = 0 \,, \end{aligned} \tag{51}$$

$$\frac{\partial \tilde{L}_2}{\partial \eta_1} = 1 - \sum_{k\in\mathbb{F}_K} \sqrt{W_k} u_k \, |v_k g_k h_k| = 0 \tag{52}$$

and

$$\frac{\partial \tilde{L}_2}{\partial \lambda_l} = P_{\max} - \varrho_l - \big(1 + r_{\text{rms}}^2 |g_l|^2 u_l^2\big) W_l - M_0 u_l^2 = 0 \,. \tag{53}$$

By similar procedure as described in Subsection III-B, we obtain the same results as given in (23), (24) and (30), because the equations (49)–(52) and (15)–(18) are pairwise the same except of the difference between τ and λ_l. On the one hand, incorporating W_l from (53) into (23), and using the same definition as in (27)–(29), lead to

$$V^{-1} = \frac{1}{r_{\text{rms}}^2} \sum_{k\in\mathbb{F}_K} \frac{\tilde{u}_k (P_{\max} - \varrho_k - \tilde{u}_k)}{(\tilde{u}_k + \alpha_k)(\tilde{u}_k + \beta_k)} \,, \tag{54}$$

which is obviously strictly decreasing with respect to each ϱ_k. Thus, the optimal value for each slack variable is zero, i.e., $\varrho_k^\star = 0$ for all $k \in \mathbb{F}_K$. On the other hand, comparing W_l from (53) with (30), leads to

$$\begin{aligned} \tilde{u}_k^\star = &\sqrt{\Big(\frac{\alpha_k \beta_k}{\alpha_k + \beta_k + P_{\max}}\Big)^2 + \frac{\alpha_k \beta_k P_{\max}}{\alpha_k + \beta_k + P_{\max}}} \\ &- \frac{\alpha_k \beta_k}{\alpha_k + \beta_k + P_{\max}} \,, \; k \in \mathbb{F}_K \,. \end{aligned} \tag{55}$$

Since equation (54) is strictly increasing in the number K of SNs and (55) holds for all SNs, we infer that all SNs are active. From (24), (29), (30), (38), (54) and (55) we thus conclude

$$V^\star = \left[\frac{P_{\max}^2}{r_{\text{rms}}^2} \sum_{k\in\mathbb{F}_K} \frac{1}{c_k^2(P_{\max}) - P_{\max}^2}\right]^{-1} , \tag{56}$$

$$u_k^\star = \sqrt{\frac{\tilde{u}_k^\star}{M_0}} \,, \; k \in \mathbb{F}_K \,, \tag{57}$$

$$W_k^\star = \frac{\tilde{u}_k^\star \alpha_k (\tilde{u}_k^\star + \beta_k)}{\alpha_k \beta_k - (\tilde{u}_k^\star)^2} \,, \; k \in \mathbb{F}_K \,, \tag{58}$$

and

$$|v_k^\star| = \frac{V^\star \tilde{u}_k^\star}{r_{\text{rms}} |h_k| \sqrt{\tilde{u}_k^\star + \beta_k} \sqrt{\alpha_k \beta_k - (\tilde{u}_k^\star)^2}} \,, \; k \in \mathbb{F}_K \,. \tag{59}$$

As mentioned in Subsection III-B, the global optimality of the obtained results is also trivially reasoned, first because of the optimization of the relaxed Lagrange function (47) with extended range of all variables, second since the global optimum point of the relaxed problem coincides with the original range of all variables, and finally there exists only a single stationary point which has a jointly convex neighborhood corresponding to a minimum and satisfying the regularity condition.

Note that by using the above results, the corresponding fusion rule cannot be simplified, since all SNs are active and they cannot thus be discarded from the fusion rule.

The equations (55)–(59) and (21) are the optimal solution of the power allocation problem only subject to the output power-range constraint per SN. They are hence the main contribution of the present subsection.

D. Comparison of the solutions

As we have shown in Subsection III-B, the SN with the smallest $c_k(P_{\text{tot}})$ consumes the whole available sum-power P_{tot}, because the combination of its sensing and communication channel is the best compared to other SNs. All other SNs do not get any transmission power, since their information reliability is too poor to be considered for data fusion. They can be discarded from the fusion rule such that the observation of the target object is less interfered by noise and consequently results in a better data communication. Note that the information reliability of each SN is only determined by the value of its corresponding $c_k(P_{\text{tot}})$.

In contrast, if the transmission power of each SN is individually limited and no sum-power constraint is given, then

This article has been accepted for publication in a future issue of this journal, but has not been fully edited. Content may change prior to final publication. Citation information: DOI 10.1109/TWC.2015.2396052, IEEE Transactions on Wireless Communications

all SNs are active and their transmission power is equal to the output power-range constraint $P_{\max}$, according to (53). In order to compare both methods from Subsection III-B and III-C, the values in (40) and (56) are needed. Note that for a fair comparison of both allocation methods in a certain scenario, an equal overall power is necessary, i.e., $P_{\text{tot}} = KP_{\max}$.

Note that $\tilde{r}$ is an unbiased estimator for each r_i due to constraint (9). By similar methods we can also minimize the mean squared error in both cases without restricting ourself to unbiased estimators. Obviously, the optimal value of V will then be smaller than that in (40) or (56).

E. Power allocation subject to both types of constraints

In the current subsection, we consider the optimization problem from Subsection III-A subject to all constraints, i.e., sum-power constraint as well as output power-range constraint per SN. Two of three different cases can be singled out and reduced to preceding instances.

First, if $KP_{\max} < P_{\text{tot}}$, then the sum-power constraint is irrelevant, because the feasible set is only limited by the output power-range constraints. Hence, the power allocation problem reduces to the one described in Subsection III-C with results given in (55)–(59) and (21). The only difference is that a part of the available sum-power remains unallocated and cannot be used.

Secondly, if $P_{\text{tot}} \leq P_{\max}$, then the output power-range constraints are irrelevant, because the feasible set is only limited by the sum-power constraint. Hence, the power allocation problem is equal to the one described in Subsection III-B. The corresponding results are described by (40)–(45) and (21).

The case of $P_{\max} < P_{\text{tot}} \leq KP_{\max}$ is most challenging. The amount of the available sum-power is possibly inadequate to supply all SNs with power $P_{\max}$. Besides, it is not possible to allocate the available sum-power only to a single SN since $P_{\max} < P_{\text{tot}}$. Hence, it will be shown that for the optimal solution only a subset of $\tilde{K} \leq K$, $\tilde{K} > 1$, SNs are active. Similar to the procedures in the previous subsections, we consider the corresponding constrained Lagrange function (relaxation with respect to the range of W_k, u_k and $|v_k|$)

$$\begin{aligned}
&L_3(W_k, u_k, v_k; \eta_1, \eta_2, \tau, \lambda_k; \xi, \varrho_k) \\
&\quad \coloneqq \sum_{k\in\mathbb{F}_K} |v_k|^2 \left(u_k^2 |h_k|^2 M_0 + N_0\right) \\
&\quad + \left(1 - \sum_{k\in\mathbb{F}_K} \sqrt{W_k} u_k \, |v_k g_k h_k| \cos(\vartheta_k + \phi_k)\right)\eta_1 \\
&\quad - \left(\sum_{k\in\mathbb{F}_K} \sqrt{W_k} u_k \, |v_k g_k h_k| \sin(\vartheta_k + \phi_k)\right)\eta_2 \\
&\quad + \left(P_{\text{tot}} - \xi - \sum_{k\in\mathbb{F}_K} \left(1 + r_{\text{rms}}^2 |g_k|^2 u_k^2\right) W_k + M_0 u_k^2\right)\tau \\
&\quad + \sum_{k\in\mathbb{F}_K} \left(P_{\max} - \varrho_k - \left(1 + r_{\text{rms}}^2 |g_k|^2 u_k^2\right) W_k - M_0 u_k^2\right)\lambda_k \,.
\end{aligned} \tag{60}$$

Since the behavior of L_3 is identical to that of L_1 and L_2 with respect to $|v_k|$ and ϑ_k, we obtain the same results for the phases as given in (21). Hence, we may modify L_3 as

$$\begin{aligned}
&\tilde{L}_3(W_k, u_k, |v_k|; \eta_1, \tau, \lambda_k; \xi, \varrho_k) \\
&\quad \coloneqq \sum_{k\in\mathbb{F}_K} |v_k|^2 \left(u_k^2 |h_k|^2 M_0 + N_0\right) \\
&\quad + \left(1 - \sum_{k\in\mathbb{F}_K} \sqrt{W_k} u_k \, |v_k g_k h_k|\right)\eta_1 \\
&\quad + \left(P_{\text{tot}} - \xi - \sum_{k\in\mathbb{F}_K} \left(1 + r_{\text{rms}}^2 |g_k|^2 u_k^2\right) W_k + M_0 u_k^2\right)\tau \\
&\quad + \sum_{k\in\mathbb{F}_K} \left(P_{\max} - \varrho_k - \left(1 + r_{\text{rms}}^2 |g_k|^2 u_k^2\right) W_k - M_0 u_k^2\right)\lambda_k \,.
\end{aligned} \tag{61}$$

Note that since the equality $\sin(\vartheta_k^\star + \phi_k) = 0$ holds due to (21), the constraint (11) is discarded in (61).

At any stationary point of $\tilde{L}_3$ the first partial derivatives of $\tilde{L}_3$ with respect to W_k, u_k, $|v_k|$, η_1, τ and λ_k must vanish, if they exist. For all $l \in \mathbb{F}_K$, this leads to

$$\frac{\partial \tilde{L}_3}{\partial W_l} = -\frac{u_l |v_l h_l g_l| \eta_1}{2\sqrt{W_l}} - \left(1 + u_l^2 r_{\text{rms}}^2 |g_l|^2\right)(\tau + \lambda_l) = 0, \tag{62}$$

$$\frac{\partial \tilde{L}_3}{\partial\, |v_l|} = 2\,|v_l| \left(u_l^2 |h_l|^2 M_0 + N_0\right) - \sqrt{W_l} u_l |h_l g_l| \eta_1 = 0\,, \tag{63}$$

$$\begin{aligned}
\frac{\partial \tilde{L}_3}{\partial u_l} &= 2|v_l|^2 u_l |h_l|^2 M_0 - \sqrt{W_l} |v_l h_l g_l| \eta_1 \\
&\quad - 2u_l \left(W_l r_{\text{rms}}^2 |g_l|^2 + M_0\right)(\tau + \lambda_l) = 0\,,
\end{aligned} \tag{64}$$

$$\frac{\partial \tilde{L}_3}{\partial \eta_1} = 1 - \sum_{k\in\mathbb{F}_K} \sqrt{W_k} u_k \, |v_k g_k h_k| = 0\,, \tag{65}$$

$$\frac{\partial \tilde{L}_3}{\partial \tau} = P_{\text{tot}} - \xi - \sum_{k\in\mathbb{F}_K} \left(1 + r_{\text{rms}}^2 |g_k|^2 u_k^2\right) W_k + M_0 u_k^2 = 0 \tag{66}$$

and

$$\frac{\partial \tilde{L}_3}{\partial \lambda_l} = P_{\max} - \varrho_l - \left(1 + r_{\text{rms}}^2 |g_l|^2 u_l^2\right) W_l - M_0 u_l^2 = 0\,. \tag{67}$$

By the same method as described in Subsection III-B, we obtain the same results as given in (23), (24) and (30), because the equations (62)–(66) and (15)–(19) are pairwise the same except of the difference between τ and $\tau + \lambda_l$. According to (67), we are able to calculate the powers W_l in terms of ϱ_l and u_l. By using the same definition as in (27)–(29) and incorporating (30), (38) and (67) into (23) and (66), we derive

$$V^{-1} = \frac{1}{r_{\text{rms}}^2} \sum_{k\in\mathbb{F}_K} \frac{1}{\left(\frac{c_k (P_{\max} - \varrho_k)}{P_{\max} - \varrho_k}\right)^2 - 1} \tag{68}$$

and

$$P_{\text{tot}} - \xi = \sum_{k\in\mathbb{F}_K} \left(P_{\max} - \varrho_k\right). \tag{69}$$

As one can see, the minimization of the signomial program in (60) is reduced to the maximization of (68) subject to (69) and $0 \leq \varrho_k \leq P_{\max} < P_{\text{tot}}$ for all $k \in \mathbb{F}_K$ with respect to each ϱ_k. Since the new maximization problem is of special structure, it is amenable to an optimal solution with the aid of

This article has been accepted for publication in a future issue of this journal, but has not been fully edited. Content may change prior to final publication. Citation information: DOI 10.1109/TWC.2015.2396052, IEEE Transactions on Wireless Communications

monotonicity and convexity of the objective (68) with respect to each $P_{\max} - \varrho_k$. The first derivative of $\frac{c_k(P)}{P}$ with respect to P leads to

$$\frac{\mathrm{d}}{\mathrm{d}P}\frac{c_k(P)}{P} = -\frac{P(\alpha_k+\beta_k)+2\alpha_k\beta_k}{2P^2\sqrt{(\alpha_k+P)(\beta_k+P)}} - \frac{\sqrt{\alpha_k\beta_k}}{P^2}\,, \quad (70)$$

which is obviously negative for all positive P. Thus, $\frac{c_k(P)}{P}$ is strictly decreasing in P, and in turn, the objective in (68) is strictly decreasing in each ϱ_k. To show the convexity more effort is needed. Since each element of the series (68) is equal to

$$\frac{1}{\left(\frac{c_k(P)}{P}\right)^2 - 1} = \frac{\left(\sqrt{\alpha_k\beta_k} - \sqrt{(\alpha_k+P)(\beta_k+P)}\right)^2 - P^2}{(\alpha_k-\beta_k)^2}, \quad (71)$$

the second derivative of each element is given by

$$\frac{\sqrt{\alpha_k\beta_k}}{2\sqrt{(\alpha_k+P)^3(\beta_k+P)^3}} > 0\,,\ P \in \mathbb{R}_+\,. \quad (72)$$

From this result, the objective in (68) is convex, and even jointly convex, with respect to each ϱ_k. Since the objective is convex and strictly decreasing with respect to each ϱ_k, a stationary point on the range $0 < \varrho_k < P_{\max}$ cannot exist. If there were a stationary point defined by $(\tilde{\varrho}_1, \tilde{\varrho}_2, \tilde{\varrho}_3, \ldots, \tilde{\varrho}_K)$, then the addition of an $\varepsilon > 0$ to the slack variable $\tilde{\varrho}_{k_1}$, which has the smallest slope among all considered slack variables, and subtraction of the same amount ε from the slack variable $\tilde{\varrho}_{k_2}$, which has the greatest slope among all considered slack variables, would lead to a greater value of the objective, because of its monotonicity and convexity. However, this would contradict the existence of a stationary point on the range $0 < \varrho_k < P_{\max}$. Hence, the optimization of the maximization problem yields a unique optimal value for each slack variable on the boundary of its feasible set. Furthermore, the optimal solution for the slack variable ξ is zero, i.e., $\xi^\star = 0$, due to increasing property of the objective (68) with respect to the number of SNs. This means that the first $\tilde{K}-1$ SNs operate on $P_{\max}$, the $\tilde{K}^{\text{th}}$ SN operates on the remaining power $P_{\text{remain}} \coloneqq P_{\text{tot}} - (\tilde{K}-1)P_{\max}$ with $0 < P_{\text{remain}} \leq P_{\max}$, while all other SNs stay idle. Consequently, the optimal power allocation method is simply described as follows.

First, all SNs are re-indexed to satisfy the inequality chain

$$c_k(P_{\max}) \leq c_{k+1}(P_{\max})\ ,\ k \in \mathbb{F}_{K-1}\,. \quad (73)$$

In turn, the first $\tilde{K}-1$ SNs are kept fix while the remaining SNs are re-indexed again to satisfy the inequality chain

$$c_k(P_{\text{remain}}) \leq c_{k+1}(P_{\text{remain}})\ ,\ k \in \mathbb{F}_{K-1} \setminus \mathbb{F}_{\tilde{K}-1}\,. \quad (74)$$

Then, we can conclude

$$\begin{aligned}(\varrho_1^\star, \ldots, \varrho_{\tilde{K}-1}^\star, \varrho_{\tilde{K}}^\star, \varrho_{\tilde{K}+1}^\star, \ldots, \varrho_K^\star)\\ = (0, \ldots, 0, P_{\max} - P_{\text{remain}}, P_{\max}, \ldots, P_{\max})\,.\end{aligned} \quad (75)$$

From (24), (29), (30), (38), (67) and (68), we infer

$$\frac{V^\star}{r_{\text{rms}}^2} = \left[\frac{1}{\left(\frac{c_{\tilde{K}}(P_{\text{remain}})}{P_{\text{remain}}}\right)^2 - 1} + \sum_{k=1}^{\tilde{K}-1}\frac{1}{\left(\frac{c_k(P_{\max})}{P_{\max}}\right)^2 - 1}\right]^{-1}, \quad (76)$$

$$\tilde{u}_k^\star = \sqrt{\left(\frac{\alpha_k\beta_k}{\alpha_k+\beta_k+P_{\max}}\right)^2 + \frac{\alpha_k\beta_k P_{\max}}{\alpha_k+\beta_k+P_{\max}}} - \frac{\alpha_k\beta_k}{\alpha_k+\beta_k+P_{\max}}\,,\ k \in \mathbb{F}_{\tilde{K}-1}\,, \quad (77)$$

$$\tilde{u}_{\tilde{K}}^\star = \sqrt{\left(\frac{\alpha_{\tilde{K}}\beta_{\tilde{K}}}{\alpha_{\tilde{K}}+\beta_{\tilde{K}}+P_{\text{remain}}}\right)^2 + \frac{\alpha_{\tilde{K}}\beta_{\tilde{K}}P_{\text{remain}}}{\alpha_{\tilde{K}}+\beta_{\tilde{K}}+P_{\text{remain}}}} - \frac{\alpha_{\tilde{K}}\beta_{\tilde{K}}}{\alpha_{\tilde{K}}+\beta_{\tilde{K}}+P_{\text{remain}}}\,, \quad (78)$$

$$u_k^\star = \sqrt{\frac{\tilde{u}_k^\star}{M_0}}\,,\ k \in \mathbb{F}_{\tilde{K}}\,, \quad (79)$$

$$W_k^\star = \frac{\tilde{u}_k^\star\alpha_k(\tilde{u}_k^\star+\beta_k)}{\alpha_k\beta_k - (\tilde{u}_k^\star)^2}\,,\ k \in \mathbb{F}_{\tilde{K}}\,, \quad (80)$$

$$|v_k^\star| = \frac{V^\star\tilde{u}_k^\star}{r_{\text{rms}}|h_k|\sqrt{\tilde{u}_k^\star+\beta_k}\sqrt{\alpha_k\beta_k - (\tilde{u}_k^\star)^2}}\,,\ k \in \mathbb{F}_{\tilde{K}}\,, \quad (81)$$

and

$$|v_k^\star| = W_k^\star = u_k^\star = 0\,,\ k \in \mathbb{F}_K \setminus \mathbb{F}_{\tilde{K}}\ . \quad (82)$$

The number $\tilde{K}$ of active SNs results from the inequality $0 < P_{\text{remain}} \leq P_{\max}$, that must be fulfilled for the last SN, and is given by the smallest integer number for which the inequality

$$\tilde{K} \geq \frac{P_{\text{tot}}}{P_{\max}} \quad (83)$$

holds.

Note that because of the same argumentation as in Subsection III-B and III-C, the global optimality of the obtained results is ensured.

Note that in the considered case, the fusion rule may be more complicated than in (46), since more SNs are active in general. On the other hand, the fusion rule may be less complicated than that from Subsection III-C, because not all SNs are possibly active.

In summary, equations (75)–(83) and (21) are the optimal solution to the power allocation problem subject to both types of constraints. They are hence the main contribution of the present subsection.

F. Discussion of the solutions

In the case $P_{\max} < P_{\text{tot}} \leq KP_{\max}$ from Subsection III-E the overall system performance is reduced because of two reasons. First, the SNR of each SN is reduced compared to the results from Subsection III-B, due to the output power-range limitation by $P_{\max} < P_{\text{tot}}$. Second, not all SNs can in general be active, due to the sum-power limitation by $P_{\text{tot}} \leq KP_{\max}$, such that the system performance is weaker compared to the results of Subsection III-C. Hence, the value in (76) is in general greater than those in (40) and (56). This behavior is not surprising and the performance reduction was predictable, since we have included more restrictions into the optimization

This article has been accepted for publication in a future issue of this journal, but has not been fully edited. Content may change prior to final publication. Citation information: DOI 10.1109/TWC.2015.2396052, IEEE Transactions on Wireless Communications

problem. To mention is, that for the general case described in Subsection III-E, we are analytically able to find relationships in closed-form between the disturbance-intensity of each SN, the geographical placement of the corresponding SN, and its operating mode, see [21] and [20] for more information.

In practice, the value of each c_k is in general unique such that the inequality chain $c_k < c_{k+1}$ for all $k \in \mathbb{F}_{K-1}$ holds. In this case, the optimal value of the objective (76) is decreasing with respect to both P_{tot} and P_{max}. If P_{max} is fixed and P_{tot} varies in the range $P_{\text{max}} \leq P_{\text{tot}} \leq KP_{\text{max}}$, then the optimal value of the objective (76) is decreasing with respect to P_{tot} because the SNR of the whole sensor network is increasing with P_{tot}. The best situation is achieved only when all SNs are active, i.e., $P_{\text{tot}} = KP_{\text{max}}$. In contrast, if P_{tot} is fixed and P_{max} varies in the range $\frac{1}{K}P_{\text{tot}} \leq P_{\text{max}} \leq P_{\text{tot}}$, then the optimal value of the objective (76) is decreasing with respect to P_{max} because the capability of each SN is increasing with P_{max}. The best situation is achieved only when a single SN is active, i.e., $P_{\text{max}} = P_{\text{tot}}$.

In a practical application, the value of P_{max} is fixed and P_{tot} can suitably be adjusted within the extended range $0 < P_{\text{tot}} \leq KP_{\text{max}}$. In order to save energy, the value of P_{tot} should be as small as possible, which means that a single SN or only a few SNs are active. On the other hand, to accurately estimate additional quantities such as position, velocity, acceleration, angle of movement, and other important properties and parameters of the target object, more than few SNs are needed to be active. Hence, if the number $\tilde{K}$ of active SNs is satisfactory in order to accurately estimate all important parameters of the target, then the best energy-aware value of P_{tot} is equal to $\tilde{K}P_{\text{max}}$. In turn, the value of P_{max} should be large enough to achieve a desired classification or detection probability. With this setup, all three system parameters $\tilde{K}$, P_{max} and P_{tot} are optimally determined for an energy-aware system design.

Note that all solutions from Subsections III-B, III-C and III-E are different to the well-known *water-filling* solution, see [22]. The difference to the water-filling solution emerges from the fact that the information flow over each effective path, consisting of a single SN, its sensing channel, the modest signal processing of the same SN, and its communication channel followed by the associated weight in the fusion center, is adjustable due to the power optimization. Thus, on the one hand, the diversity of each effective path is not predetermined such that the water-filling solution cannot hold in its general form. On the other hand, the diversity of best effective paths is amplified in comparison to the diversity of poorest effective paths because of the optimal solution to the power allocation.

G. Numerical verification

The main difficulty of dealing with optimization problems like (13), (47) and (60) is the absence of a specific mathematical structure, e.g., monotonicity, convexity and higher order properties. In order to prove or show global optimality, a considerable effort is thus needed for all aforementioned optimization problems, see [23]. In this subsection we present an equivalent numerical method to verify our previous analytical solutions in a simple way. In particular, the optimization problem considered in (60) is rewritten such that to obtain a sequential convex program (SCP), which in turn can easily be solved by standard numerical tools like MATLAB® [24] with the aid of CVX [25]. Our approach is based on the substitution of all variables by

$$u_k = \mathrm{e}^{u'_k}\,,\ |v_k| = \mathrm{e}^{v'_k}\,,\ |w_k| = \mathrm{e}^{w'_k}\,, \tag{84}$$

where all new variables are real valued. Then an equivalent optimization problem of (61) is given by

$$\begin{aligned}
\underset{u'_k, v'_k, w'_k \in \mathbb{R}}{\text{minimize}} \ & \sum_{k\in\mathbb{F}_K} \mathrm{e}^{2v'_k}\big(\mathrm{e}^{2u'_k}|h_k|^2 M_0 + N_0\big)\,, \\
\text{s.t.} \ & \sum_{k\in\mathbb{F}_K} \mathrm{e}^{u'_k+v'_k+w'_k}\,|g_k h_k| = 1\,, \\
& \sum_{k\in\mathbb{F}_K} \big(1 + r^2_{\text{rms}}|g_k|^2\mathrm{e}^{2u'_k}\big)\mathrm{e}^{2w'_k} + M_0\mathrm{e}^{2u'_k} \leq P_{\text{tot}}\,, \\
& \big(1 + r^2_{\text{rms}}|g_k|^2\mathrm{e}^{2u'_k}\big)\mathrm{e}^{2w'_k} + M_0\mathrm{e}^{2u'_k} \leq P_{\text{max}}\ \forall k\,,
\end{aligned} \tag{85}$$

where the equality constraint is not an affine function. To convexify the above problem, we linearize the equality constraint and obtain the SCP

$$\begin{aligned}
\underset{u'_{k,n}, v'_{k,n}, w'_{k,n}}{\text{minimize}} \ & \sum_{k\in\mathbb{F}_K} \mathrm{e}^{2v'_{k,n}}\big(\mathrm{e}^{2u'_{k,n}}|h_k|^2 M_0 + N_0\big)\,, \\
\text{s.t.} \ & \sum_{k\in\mathbb{F}_K} \mathrm{e}^{\delta_{k,n-1}}\big(1 + \delta_{k,n} - \delta_{k,n-1}\big)\,|g_k h_k| = 1\,, \\
& \sum_{k\in\mathbb{F}_K} \big(1 + r^2_{\text{rms}}|g_k|^2\mathrm{e}^{2u'_{k,n}}\big)\mathrm{e}^{2w'_{k,n}} + M_0\mathrm{e}^{2u'_{k,n}} \leq P_{\text{tot}}\,, \\
& \big(1 + r^2_{\text{rms}}|g_k|^2\mathrm{e}^{2u'_{k,n}}\big)\mathrm{e}^{2w'_{k,n}} + M_0\mathrm{e}^{2u'_{k,n}} \leq P_{\text{max}}\ \forall k\,,
\end{aligned} \tag{86}$$

where the auxiliary variable $\delta_{k,n} \coloneqq u'_{k,n} + v'_{k,n} + w'_{k,n}$ is used. The counting index $n \in \mathbb{N}$ represents thereby the n^{th} solution of the SCP (86) with arbitrary feasible initial-values $u'_{k,0}$, $v'_{k,0}$ and $w'_{k,0}$. The value of the objective after the n^{th} iteration is denoted by V_n. For sufficiently large n and an accurate choice of initial-values, we expect that the solution of (86) converges to the solutions derived in Subsection III-E which means $V_n \underset{n\mapsto\infty}{\longrightarrow} V^\star$. In the next section we will discuss these solutions.

IV. Sensitivity Analysis and Numerical Results

In this section, we first compare the analytical solution of the objective (76) with the numerical computation of the equivalent SCP (86). Afterwards, we simulatively investigate the behavior of the optimal value in (76) with respect to $\sigma_g^2 \coloneqq \mathcal{E}[|g_k|^2]$, $\sigma_h^2 \coloneqq \mathcal{E}[|h_k|^2]$, M_0 and N_0. Subsequently, we analyze the sensitivity of a sensor network, which is indeed designed by the optimal power allocation strategy from Subsection III-E, but with an imperfect knowledge of the actual channel-state. In particular, we investigate different independent cases, where both estimates $\hat{g}_k \coloneqq g_k + \Delta g_k$ and $\hat{h}_k \coloneqq h_k + \Delta h_k$ are used instead of g_k and h_k, respectively, in order to re-design the sensor network. We compare then the optimal value in (76) of the sensor network with optimal known parameters to the conditional mean square error (MSE)

$$\hat{V} \coloneqq \mathcal{E}\big[|\tilde{r} - r_i|^2 \mid \Delta g_k, \Delta h_k\big] \tag{87}$$

This article has been accepted for publication in a future issue of this journal, but has not been fully edited. Content may change prior to final publication. Citation information: DOI 10.1109/TWC.2015.2396052, IEEE Transactions on Wireless Communications

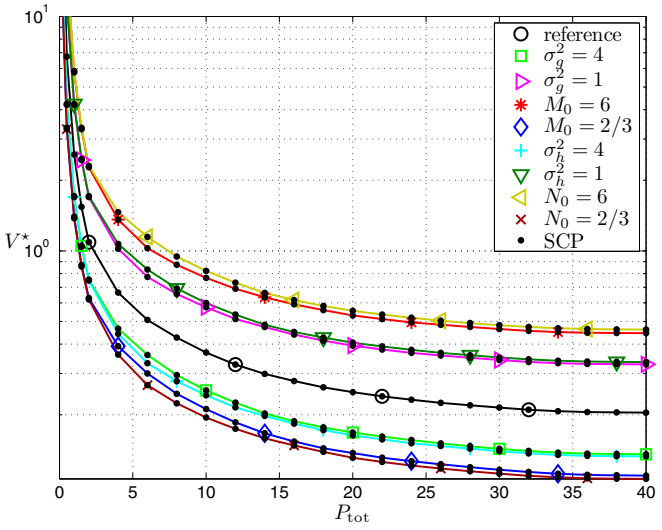

Fig. 3. The behavior of $V^\star$ from equation (76) with respect to P_{tot} is visualized together with the numerical results obtained by computation of the SCP (86). All curves show a decreasing property in P_{tot}. The reference curve has the default parameters $\sigma_g^2 = 2$, $\sigma_h^2 = 2$, $M_0 = 2$ and $N_0 = 2$. The results of the SCP for sufficiently large number of iterations are equivalent to the closed-form solutions.

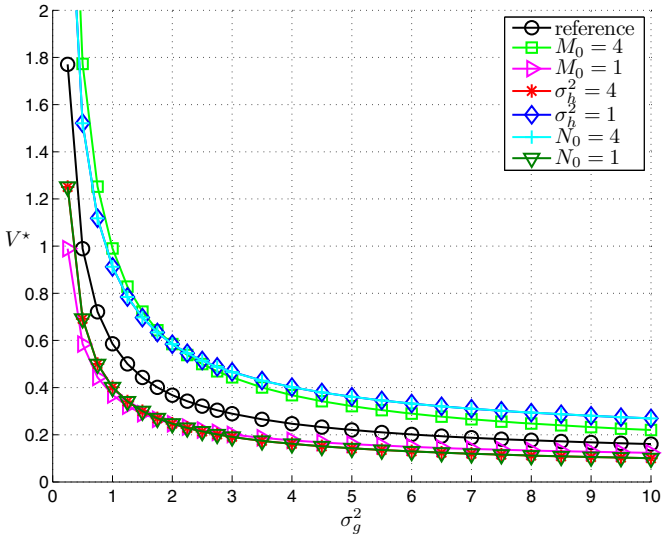

Fig. 4. Behavior of $V^\star$ with respect to σ_g^2. All curves show a decreasing property in σ_g^2. The reference curve has the default parameters $\sigma_h^2 = 2$, $M_0 = 2$ and $N_0 = 2$.

of the same re-designed sensor network with imperfect information. In general, the estimate $\tilde{r}$ in (87) is biased compared to the case with perfect information, i.e., $\mathcal{E}[\tilde{r} - r_i] \neq 0$. In addition, the selection of most reliable SNs is no longer ensured. Hence, the value in (87) is mostly greater than that of (76), see also the definition (12). Furthermore, due to inaccurate knowledge of sensing and communication channels, the given power constraints may be violated in the erroneous design. All these effects are equivalently relevant for a discussion and comparison. Since an analytical comparison seems to be out of reach, we set out to use numerical methods to obtain the sensitivity analysis and visualize corresponding simulation results.

In order to fairly compare all results, we simulate a *reference* curve for each figure. All reference curves are based on parameters under consideration with default values given in Table II. Unless otherwise stated, we usually create a new curve only by changing the value of a single parameter. The specific new value of that parameter is noted in the legend of the corresponding figure.

TABLE II
DEFAULT VALUES USED FOR EACH REFERENCE CURVE.

K	r_{rms}^2	σ_g^2	σ_h^2	$\sigma_{\Delta g}^2$	$\sigma_{\Delta h}^2$	M_0	N_0	$P_{\max}$	P_{tot}
20	1	2	2	0	0	2	2	2	10

A. Verification of analytical and numerical solutions

In Figure 3, both analytical and numerical results for the optimal objective respectively obtained by (76) and (86) are presented. The SCP is calculated with three criteria of termination. The first one is a minimum number of iterations $n \geq 8$. The second criterion is a feasibility check, fulfilled by $|1 - \sum_{k \in \mathbb{F}_K} \mathrm{e}^{\delta_{k,n-1}} \left(1 + \delta_{k,n} - \delta_{k,n-1}\right) |g_k h_k| \,| \leq 10^{-4}$. The last one is a check of convergency and is determined by the relative value condition $|V_n - V_{n-5}| \leq V_n \cdot 10^{-3}$. All above criteria are based on experience in this field. Furthermore, each SCP point is calculated with three randomly and independently generated initial-values, where at the end of each three runs the best achieved result is depicted. Since the precision of the numerical solutions are very high, due to the strict termination criteria from above, all SCP points fall onto the analytical curves. This coincidence reinforces the statement for global optimality of the analytical results on the one hand, and the convergence of the numerical method on the other hand.

Since the solution of the SCP in (86) is highly computationally intensive and its results do not show any additional information, we omit this computation and its corresponding results in the remaining part of this paper.

B. Behavior of $V^\star$

By considering (38) we see that the disturbance-intensity $c_k(P)$ is symmetric in α_k and β_k and hence the optimum value $V^\star$ in (76) is also symmetric in each α_k and β_k. Thus, changing the roles of each pair g_k and M_0 with each pair h_k and N_0 results in the same value for $V^\star$ while keeping $r_{\text{rms}} = 1$ constant. Because of this fact it is enough to investigate the behavior of $V^\star$ only with respect to σ_g^2 and M_0 while σ_h^2, N_0 and r_{rms} are kept constant. All random processes g_k, h_k, Δg_k, Δh_k, m_k and n_k are randomly generated with zero mean Gaussian distributions for each simulation step. The random process r_i is randomly generated with a uniform distribution on $\{-1, 1\}$ in each simulation step. All other parameters are kept constant. We apply a Monte-Carlo simulation, where the number of parameter realizations for each simulation point is always 100000. The same simulation setup is also applied for all results in the next subsection.

In Figure 4, the decreasing property of $V^\star$ with respect to the variance σ_g^2 of all sensing channels is shown. The reason

This article has been accepted for publication in a future issue of this journal, but has not been fully edited. Content may change prior to final publication. Citation information: DOI 10.1109/TWC.2015.2396052, IEEE Transactions on Wireless Communications

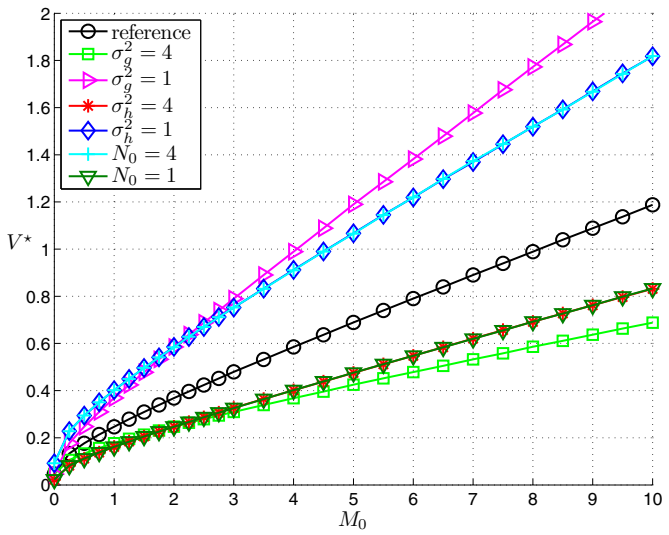

Fig. 5. Behavior of $V^\star$ with respect to M_0. All curves show an increasing property in M_0. The reference curve has the default parameters $\sigma_g^2 = 2$, $\sigma_h^2 = 2$ and $N_0 = 2$.

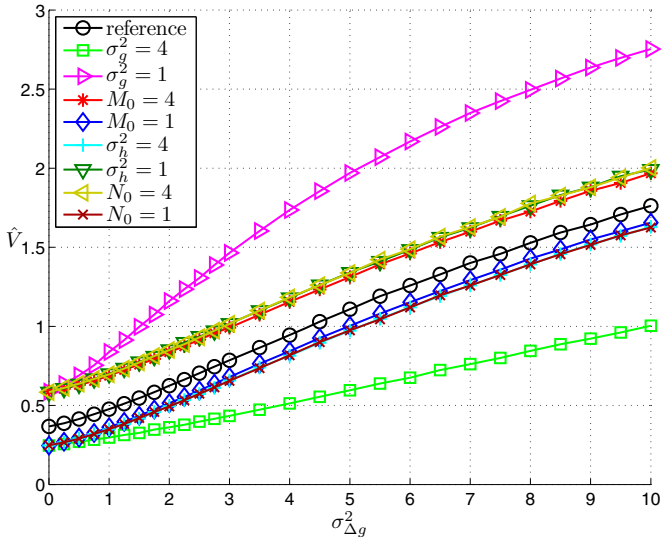

Fig. 6. Behavior of $\hat{V}$ with respect to $\sigma_{\Delta g}^2$. All curves show an increasing property in $\sigma_{\Delta g}^2$. The reference curve has the default parameters $\sigma_g^2 = 2$, $\sigma_h^2 = 2$, $M_0 = 2$ and $N_0 = 2$.

behind the decreasing property is that the whole network observes the target object more reliable in case where the variance of sensing channels is higher. Furthermore, it can be seen that increasing N_0 has an equivalent effect on the objective as decreasing σ_h^2 and vice versa. It is also interesting to note that the objective shows highest sensitivity to the variation of M_0 when the sensing channel is rather weak (small σ_g^2). The observed sensitivity is illustratively reduced for higher variances of the sensing channel. Furthermore, the objective attains a more or less constant value for very high variances of the sensing channel. The reason is that the resulted objective is dominated by the quality of the communication channel when the sensing channel gets stronger.

In Figure 5 it is shown that in contrast to the curves in Figure 4, the property of $V^\star$ is increasing with respect to the noise power M_0. For small values of M_0 all curves have a square root property while for large values of M_0 all curves behave linear. The deviation of all curves is greater for large values of M_0 than for small values. Furthermore, the value of M_0 has more impact on the deviation of $V^\star$ caused by σ_g^2 than by other parameters, as mentioned before. As already described for Figure 4, increasing N_0 is equivalent to decreasing σ_h^2 and vice versa.

C. Sensitivity of $\hat{V}$

A sensitivity analysis of $\hat{V}$ is very important in order to justify assumptions concerning the channel-state knowledge. In Figure 6, we consider the case where the error variance $\sigma_{\Delta g}^2 := \mathcal{E}[|\Delta g_k|^2]$ of estimated sensing channels is greater than or equal to zero. In the case where $\sigma_{\Delta g}^2$ is equal to zero, the identity $\hat{V} = V^\star$ holds. Otherwise, $\hat{V}$ is always greater than $V^\star$, i.e., $\hat{V}(\sigma_{\Delta g}^2) \geq \hat{V}(0)$. All curves pass through three different regions whereas only the first and the second region are visible in Figure 6. In the first region, i.e., for low values of $\sigma_{\Delta g}^2$, all curves are slowly increasing. The selection of most reliable SNs is still mostly ensured in the first region while the optimal power allocation is no longer insured. In the second region, i.e., for mid-range values of $\sigma_{\Delta g}^2$, all curves are rapidly increasing since the correct sensor selection gets out of control. In the last region, i.e., for high values of $\sigma_{\Delta g}^2$, all curves are linearly increasing. In this region the optimal sensor selection almost always fails. This means that SNs are randomly selected and the allocated power is also random. The increasing property (not constant) of all curves in the third region is comparable with the increasing property in the first region, because the roles of g_k and Δg_k are exchanged. The system is then designed by Δg_k instead of g_k and thus g_k itself acts as an estimation error of Δg_k. In summary, the best operation region of the proposed system is the first region in which $\sigma_{\Delta g}^2 \ll \sigma_g^2$ holds, while a system operation in the third region, for which $\sigma_{\Delta g}^2 \gg \sigma_g^2$ holds, should be avoided.

As can also be seen, the deterioration of the performance is not only amplified by high noise powers M_0 and N_0, but also by low channel variances σ_g^2 and σ_h^2. The form of the curves is mainly dominated and prescribed by the channel variance σ_g^2. All curves in the middle of the figure run almost parallel because the variance σ_g^2 of all those curves is the same.

V. Conclusion

The main contribution of the present work is to present an optimal solution to the power allocation problem in distributed active multiple-radar systems subject to different power constraints. We have introduced a system model, a linear fusion rule and a simple objective function, which enable us to solve the power allocation problem analytically. Three different cases of power constraints have been investigated. For a limitation of transmission power per sensor node and a sum-power limitation as well as their combination, we have analytically obtained optimal solutions in closed-form. Furthermore, all proposed solutions are valid for AWGN channels as well as

for frequency-flat slow-fading channels, provided that channel state information is available at each receiver. In addition, we have discussed the sensitivity of the derived optimal power allocation with respect to perfect and imperfect parameter knowledge. In this way, we have shown that the optimal power allocation is robust against small inaccuracies in the channel state information.

ACKNOWLEDGMENT

This work was assisted by Dipl.-Ing. Johannes Schmitz, Institute for Theoretical Information Technology, RWTH Aachen University. We would like to thank him for his effort and commitment. We also want to thank all anonymous reviewers for their fruitful discussions.

REFERENCES

[1] R. Srinivasan, "Distributed radar detection theory," *IEE Proceedings-F*, vol. 133, no. 1, pp. 55–60, Feb 1986.

[2] A. L. Hume and C. J. Baker, "Netted radar sensing," in *Proc. IEEE Int. Radar Conf.*, 2001, pp. 23–26.

[3] L. Pescosolido, S. Barbarossa, and G. Scutari, "Radar sensor networks with distributed detection capabilities," in *Proc. IEEE Int. Radar Conf.*, May 2008, pp. 1–6.

[4] Y. Yang, R. S. Blum, and B. M. Sadler, "A distributed and energy-efficient framework for Neyman-Pearson detection of fluctuating signals in large-scale sensor networks," *IEEE J. Sel. Areas Commun.*, vol. 28, pp. 1149–1158, Sep 2010.

[5] G. Alirezaei and R. Mathar, "Channel capacity related power allocation for distributed sensor networks with application in object classification," in *International Conference on Computing, Networking and Communications (ICNC'13)*, San Diego, California, USA, Jan. 2013, pp. 502–507.

[6] S. Gezici, Z. Tian, G. B. Giannakis, H. Kobayashi, A. F. Molisch, H. V. Poor, and Z. Sahinoglu, "Localization via ultra-wideband radios: A look at positioning aspects for future sensor networks," *IEEE Signal Process. Mag.*, vol. 22, pp. 70–84, Jul 2005.

[7] C. Debes, J. Riedler, A. M. Zoubir, and M. G. Amin, "Adaptive target detection with application to through-the-wall radar imaging," *IEEE Trans. Signal Process.*, vol. 58, no. 11, pp. 5572–5583, 2010.

[8] G. Alirezaei and R. Mathar, "Power allocation for power-limited sensor networks with application in object classification," in *Global Information Infrastructure Symposium (GIIS'12)*, Choroní, Venezuela, Dec. 2012, pp. 1–5.

[9] G. Alirezaei, M. Reyer, and R. Mathar, "Optimum power allocation in sensor networks for passive radar applications," *IEEE Transactions on Wireless Communications*, vol. 13, no. 6, pp. 3222–3231, Jun. 2014.

[10] G. Alirezaei and R. Mathar, "Optimum power allocation for sensor networks that perform object classification," *IEEE Sensors Journal*, vol. 14, no. 11, pp. 3862–3873, Nov. 2014.

[11] R. O. Duda, P. E. Hart, and D. G. Stork, *Pattern Classification*, 2nd ed. John Wiley & Sons, Inc, 2000.

[12] A. Lapidoth, *A Foundation in Digital Communication*. Cambridge University Press, 2009.

[13] M. Chiang, *Geometric Programming for Communication Systems*. Princeton: now Publishers Inc., 2005.

[14] S. Boyd and L. Vandenberghe, *Convex Optimization*. California: Cambridge University Press, 2004.

[15] D. G. Luenberger and Y. Ye, *Linear and Nonlinear Programming*, 3rd ed. Springer Science+Business Media, 2008.

[16] D. P. Bertsekas, *Nonlinear Programming*, 2nd ed. Athena Scientific, 1999.

[17] D. G. Luenberger, *Optimization by Vector Space Methods*, 1st ed. John Wiley & Sons, Inc., 1969.

[18] E. Hansen and G. W. Walster, *Global Optimization Using Interval Analysis*, 2nd ed. Marcel Dekker Inc., 2003.

[19] D. W. Peterson, "A review of constraint qualifications in finite-dimensional spaces," *SIAM Review*, vol. Vol. 15, no. No. 3, pp. 639–654, July 1973.

[20] G. Alirezaei, *Optimizing Power Allocation in Sensor Networks with Application in Target Classification*, ser. Berichte aus der Kommunikationstechnik. Aachen, Germany: Shaker Verlag, Sep. 2014.

[21] G. Alirezaei and J. Schmitz, "Geometrical sensor selection in large-scale high-density sensor networks," in *The IEEE International Conference on Wireless for Space and Extreme Environments (WiSEE'14)*, Noordwijk, Netherlands, Oct. 2014.

[22] S. Stańczak, M. Wiczanowski, and H. Boche, *Fundamentals of Resource Allocation in Wireless Networks: Theory and Algorithms*, 2nd ed. Berlin: Springer, 2008.

[23] R. Horst and H. Tuy, *Global Optimization: Deterministic Approaches*, 2nd ed. Springer-Verlag, 1992.

[24] MATLAB, *version 7.11.0.584 (R2010b)*. Natick, Massachusetts: The MathWorks Inc., 2010.

[25] M. Grant and S. Boyd, "CVX: Matlab software for disciplined convex programming, version 2.1," http://cvxr.com/cvx, Mar. 2014.